Spatio-temporal Stability Analysis of Falling Film Over Heated Inclined Plane

Arnab Choudhury and Arghya Samanta

Abstract Linear stability analysis of a thin liquid film falling down a uniformly heated slippery inclined plane has been performed. The spatial growth rates for thermocapillary P mode and S mode have been estimated by solving a coupled set of boundary value problems employing Chebyshev spectral collocation method. Marangoni number is found to destabilize both the P mode and S mode, and Biot number seems to have a dual influence on the S mode instability. The S mode gets stabilized with the increase in spanwise wavenumber, whereas the P mode gets destabilized. The hydrodynamic shear mode has also been captured analytically for inviscid flow, which indicates a slight stabilizing effect of Marangoni number on it.

Keywords Thin film flow · Hydrodynamic instability · Thermocapillary instability

1 Introduction

Thin film flows are encountered in several engineering and scientific applications such as thermal protection of rocket engines, cooling of semiconductors, heat transfer in condensers and evaporators, etc. Therefore, it is of particular interest to study the instabilities in heated thin film flows as it affects the interfacial heat transfer significantly. The linear stability of a thin film flow down an uniformly heated inclined plane has been studied by Lin [7]. He has analytically predicted the critical Reynolds number as a function of Marangoni number and inclination angel for hydrodynamic surface mode of instability. Lin [6] has also shown the existence of hydrodynamic shear mode in the falling film flow and predicted the critical Reynolds number for it. Goussis and Kelly [3] have examined the influence of Marangoni number on thermocapillary P mode and S mode. Incorporating energy budget analysis, they have also suggested some mechanisms by virtue of which the S mode, P mode, and H mode instability triggers. The influence of Soret number on the temporal and spatial stability of a heated binary film has been studied by Hu et al. [4]. The thermocaillary

A. Choudhury (✉) · A. Samanta
Department of Applied Mechanics, IIT Delhi, Hauz Khas, New Delhi 110016, India
e-mail: arnab.choudhury@am.iitd.ac.in

P mode has been partially captured for low values of streamwise wavenumber in this study. Samanta [9] has deciphered the effect of electric field on the shear mode instability. He has found a stabilizing effect of applied electric field intensity on shear mode. The effect of different flow parameters on the shear mode at inviscid limits has also been analysed. Pascal and D'Alessio [8] have analysed the linear stability of a heated binary film flow where the density of the liquid film varies with respect to temperature. The influence of Marangoni number at low Reynolds number on surface and S modes of instability have been examined. Bhat and Samanta [1] have carried out a linear stability analysis of a falling film having insoluble surfactant contamination. They have examined the effect of different parameters on the hydrodynamic surface mode and shear mode. They have also performed the inviscid analysis where they have shown a stabilizing influence of slip on shear mode. Choudhury and Samanta [2] have performed the temporal stability of a heated falling film down a slippery incline. The authors have performed a detailed parametric study on four different instability modes i.e., H mode, P mode, S mode, and shear mode.

From these literatures, it can be observed that there exist several studies regarding the temporal stability of all the four modes of instability, that is, H mode, S mode, P mode and shear mode. The studies of spatial stability is also performed for H mode and shear mode only. But there are no studies found regarding the spatial stability of thermocapillary P mode and S mode. Our aim for the present study is to provide these missing links in the present literature.

2   Mathematical Formulation

Consider a viscous liquid thin film falling under the action of gravity down an incline as shown in Fig. 1. The inclined plane is maintained at a uniform temperature T_w which is higher than the ambient temperature T_a and it makes angle θ with the horizon. All the thermophysical properties of the fluid such as viscosity (μ), density (ρ), thermal conductivity (κ) etc. are kept constant for carrying out the linear stability analysis. Although the surface tension (σ) is considered to vary with temperature according to the relation (1) as we are interested to study the thermocapillary modes of instability.

$$\sigma(T) = \sigma_0 - \varepsilon(T - T_a), \tag{1}$$

where, σ_0 denotes the surface tension at ambient conditions and $\varepsilon = -\frac{d\sigma}{dT}\big|_{T=T_a} > 0$. The Cartesian coordinate system is considered to originate from the slippery plane and the orientation of it is shown in Fig. 1. The film thickness corresponding to the base flow is d, and $h(x, z, t)$ denotes the thickness of the perturbed liquid film. Now following the work of Choudhury and Samanta [2] we can formulate the Orr-Sommerfeld type boundary value problem (OS-BVP)

$$\left(D^2 - k^2\right)^2 \hat{\phi} = i\mathrm{Re}\left[\left(k_x \overline{U} - \omega\right)\left(D^2 - k^2\right) + \frac{2k_x}{1 + 2\beta}\right]\hat{\phi}, \quad y \in [0, 1], \quad (2)$$

$$\left(D^2 - k^2\right)\hat{\tau} = \mathrm{Pe}\left[i\left(k_x \overline{U} - \omega\right)\hat{\tau} - \left(\frac{\mathrm{Bi}}{1 + \mathrm{Bi}}\right)\hat{\phi}\right] = 0, \quad y \in [0, 1], \quad (3)$$

$$\hat{\phi} = 0, \ \hat{\tau} = 0, \ D\hat{\phi} - \beta D^2 \hat{\phi} = 0, \quad \text{at } y = 0, \quad (4)$$

$$\left(D^2 + k^2\right)\hat{\phi} + 2k^2 Ma\left[\hat{\tau} - \frac{\mathrm{Bi}\hat{\eta}}{1 + \mathrm{Bi}}\right] + \frac{2ik_x\hat{\eta}}{1 + 2\beta} = 0, \quad \text{at } y = 1, \quad (5)$$

$$\left[D^2 - i\mathrm{Re}(k_x - \omega) - 3k^2\right]D\hat{\phi} - 2\hat{\eta}k^2$$
$$\times \left[\frac{\cot\theta}{1 + 2\beta} - k^2\left(\frac{Ma}{1 + \mathrm{Bi}} - We\right)\right] = 0, \quad \text{at } y = 1 \quad (6)$$

$$D\hat{\tau} - \mathrm{Bi}\left[\frac{\mathrm{Bi}\hat{\eta}}{1 + \mathrm{Bi}} - \hat{\tau}\right] = 0, \quad \text{at } y = 1, \quad (7)$$

$$\hat{\phi} - i(k_x - \omega)\hat{\eta} = 0, \quad \text{at } y = 1, \quad (8)$$

where D stands for the differential operator $\frac{d}{dy}$. In Eqs. (2)–(8), $\hat{\phi}$, $\hat{\tau}$, and $\hat{\eta}$ denotes the amplitude of perturbation velocity, perturbation temperature and perturbation film thickness. The imposed disturbances to the perturbation quantities are considered to be in normal mode form, where $\omega = \omega_r + i\omega_i$ denotes the angular frequency and $k = \sqrt{k_x^2 + k_z^2}$ is the wave number. In this case, k_x and k_z are streamwise and spanwise wavenumbers, respectively. Again the complex spanwise wavenumber can be represented as $k = k_r + ik_i$, where $-k_i$ is the spatial growth rate. The angular frequency ω remains real while calculating the spatial growth rate. The temporal growth rate is denoted by ω_i and the wavenumber k remains real while calculating temporal growth rate. In the OS-BVP (2)–(8), Re, Ma, Bi, Pe, We denotes Reynolds number, Marangoni number, Biot number, Peclet number, and Weber number respectively. Again Peclet number can be written as $\mathrm{Pe} = \mathrm{Re}\,\mathrm{Pr}$ where Pr denotes Prandtl number. The dimensionless slip length and base flow velocity is denoted by β and $\overline{U} = \left(2y - y^2 + 2\beta\right)\big/(1 + 2\beta)$. To capture the effect of Marangoni number and Biot number on the S mode and P mode instability properly we will use the transformations: $M = \mathrm{Ma}(1 + 2\beta)^{1/3}(2\mathrm{Re})^{2/3}$, $\mathrm{Bi} = B(2\mathrm{Re})^{1/3}/(1 + 2\beta)^{1/3}$, and $\mathrm{Ka} = \mathrm{We}(1 + 2\beta)^{1/3}(2\mathrm{Re})^{2/3})^{2/3}$. Here Ka denotes the Kapitza number.
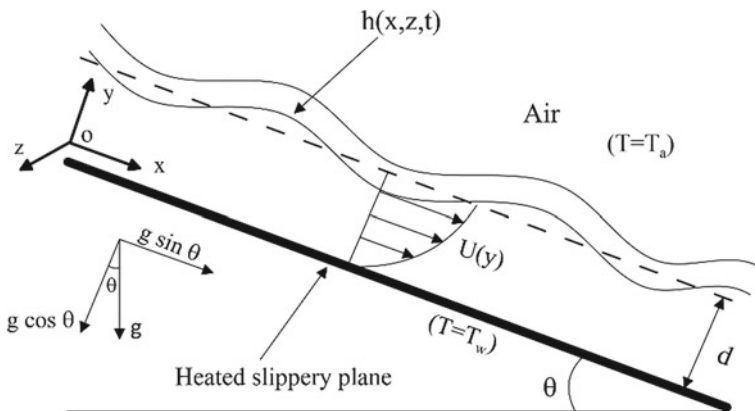
Fig. 1 Schematic of uniformly heated falling film

# 3 Results and Discussion

3.1 Spatial Stability Analysis

3.1.1 Validation

The Eigen value problem (2)–(8) have been solved numerically incorporating Chebyshev spectral collocation method. To check the consistency of the present numerical code, we have verified the present results with the existing results in literature. In Fig. 2, the neutral stability curve corresponding to H mode and S mode instability has been shown for $M = 15$ and $M = 30$ when $B = 1$, Ka $= 250$, $k_z = 0$, $\beta = 0$, $\theta = 15°$, and Pr $= 7$. It can be clearly observed that present numerical code reproduces the results of Kalliadasis et al. [5] quiet accurately. In this case, at lower value of M, we get two separate neutral curves for hydrodynamic H mode and thermocapillary S mode of instability. But as the Marangoni number Ma, or equivalently M increases, both the modes merge and forms a single neutral stability curve.

3.1.2 Influence of Marangoni Number

Here, we shall discuss the independent influence of Marangoni number, or equivalently M on the spatial growth rate of thermocapillary P mode and S mode which have been captured numerically. The modes are been distinguished from each other on the basis of their phase speed. Note that from now onwards all the numerical results are produced keeping the parameters Ka $= 240$, Pr $= 6.5$, $\theta = 15°$ and $\beta = 0.03$ fixed. In Fig. 3a, the spatial growth rate for S mode have been plotted in (k_r, k_i) plane for $M = 14$, $M = 10$, and $M = 6$ when Re $= 0.1$, $B = 1$, and $k_z = 0$. The spatial growth rate is found to be increasing with the increase in M for S mode instability. The S

Fig. 2 Evolution of neutral stability curves for $M = 15$ and $M = 30$ when $B = 1$, Ka $= 250$, $k_z = 0$, $\beta = 0$, $\theta = 15°$, and Pr $= 7$. Black and Blue lines represent $M = 15$, and $M = 30$ respectively. The results from Kalliadasis et al. [5] are represented by symbolic points
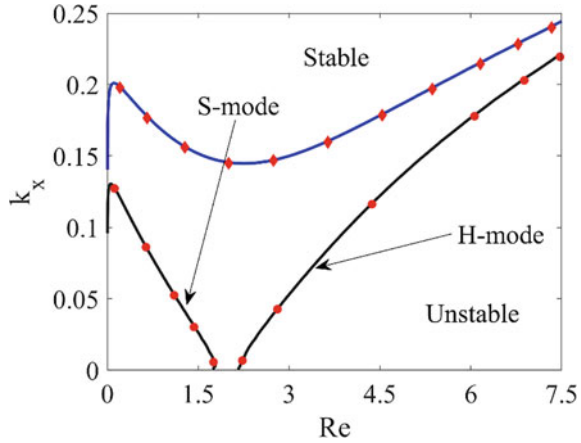
mode instability triggers at low Reynolds number due to the surface tension gradient imposed by non-uniform temperature distribution at the liquid–air interface. As M increases, the surface tension gradient also increases between crest and trough of the waves at free surface resulting in a destabilizing effect on the flow. It is interesting to note that with the increase in Reynolds number the S mode instability gets stabilized as inertia force takes over the Marangoni force. Now the independent effect of M on the P mode will be analysed. The spatial growth rates related to P mode in (k_r, k_i) plane have been shown in Fig. 3b for $M = 20$, $M = 21$, and $M = 22$ when Re $= 10$, $B = 1$, and $k_z = 0$. Now, from Fig. 3b, it can be clearly observed that as the value of M increases the spatial growth rate also increases significantly. Hence, we may conclude that M or equivalently Ma destabilizes the P mode instability. It can also be observed that the P mode instability is found at the short wave regime unlike the S mode instability, which can only be present at long wave regime.

3.1.3 Influence of Biot Number

Now the influence of Biot number on the spatial growth rate of S mode and P mode will be discussed. Interestingly, we have found a dual effect of Biot number Bi or, equivalently B on the S mode depending upon the range of B. In Fig. 4a the evolution of spatial growth rate $-k_i$ has been plotted against the real part of streamwise wave number k_r at small values of B ($B \leq 0.75$) when $M = 17$, Re $= 0.1$, and $k_z = 0$. At lower range of B, it can be noticed that B imparts a destabilizing effect on the S mode. On the contrary, at the higher values of B ($B \geq 0.75$) it may be noticed that with the increase in the value of B, the spatial growth rate decreases as shown in Fig. 4b. Therefore we may conclude that B has a stabilizing effect on S mode at higher range of B. This phenomenon can be attributed to the fact that with the increment in B, the relative heat transfer increases, resulting in lower temperature of free surface and hence stabilizing the S mode.
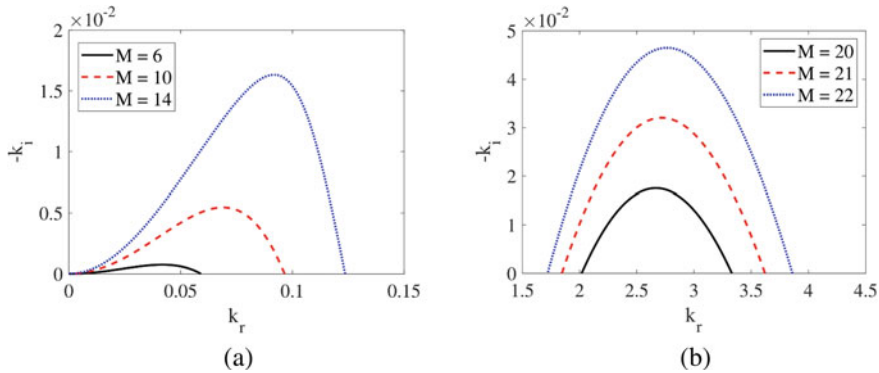
Fig. 3 **a** Evolution of spatial growth rate $-k_i$ for the S mode in (k_r, k_i) plane when Re $= 0.1$. **b** Evolution of spatial growth rate $-k_i$ for the P mode in (k_r, k_i) plane when Re $= 10$. The parameters $B = 1$ and $k_z = 0$ are kept constant
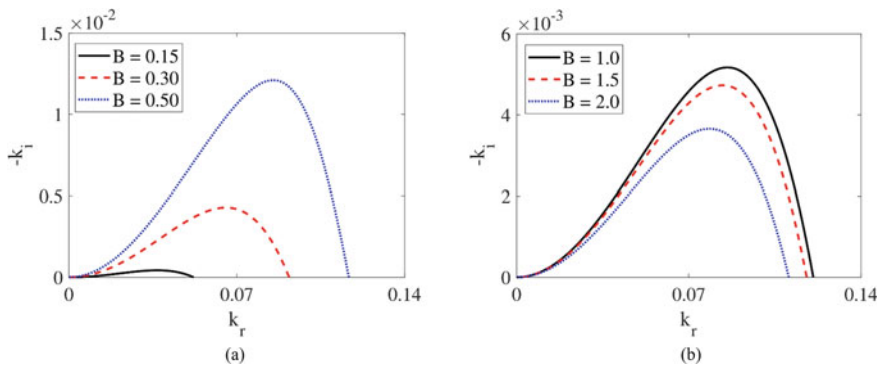
Fig. 4 **a** Evolution of spatial growth rate $-k_i$ for the S mode in (k_r, k_i) plane when Re $= 0.1$. **b** Evolution of spatial growth rate $-k_i$ for the S mode in (k_r, k_i) plane when Re $= 0.4$. The parameters $M = 17$ and $k_z = 0$ are kept constant

Now we will decipher the solo influence of Biot number on the P mode. The P mode instability is basically triggered by the steady convection rolls within the flow which is formed due to the surface tension gradient at the liquid–air interface. The variation of spatial growth rate k_i with respect to real part of streamwise wavenumber has been shown in Fig. 5 for $B = 1$, $B = 1.25$, and $B = 1.5$, when Re $= 10$, $M = 21$, and $k_z = 0$. It can be noticed that with the increase in B the spatial growth rate for P mode decreases significantly. Hence we may conclude that Biot number stabilizes the thermocapillary P mode.

Fig. 5 Evolution of spatial growth rate $-k_i$ for the P mode in (k_r, k_i) plane when Re $= 10$, $M = 21$, and $k_z = 0$
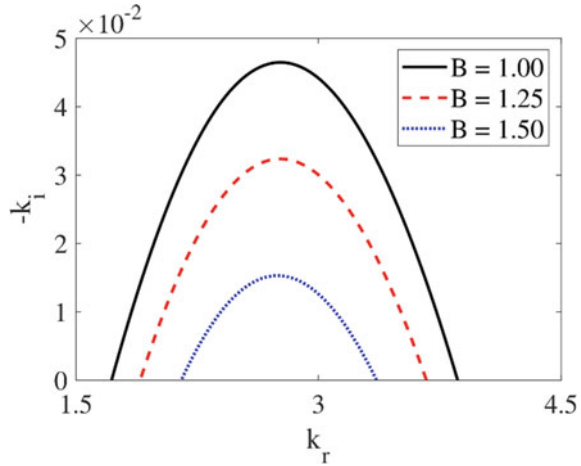

3.1.4 Influence of Spanwise Wavenumber

In this section the independent effect of spanwise wavenumber on both S mode and P mode instability will be deciphered. In Fig. 6a the spatial growth rates corresponding to S mode have been plotted in (k_r, k_i) plane for $k_z = 0.1$, $k_z = 0.05$, and $k_z = 0$ when Re $= 1$, $M = 25$, and $B = 1$. It can be observed that the maximum spatial growth rate for S mode reduces with the increase in k_z. The onset of stability for the S mode also decreases significantly with the increase in k_z. Therefore it may be concluded that spanwise wavenumber has a stabilizing influence on the S mode instability. It is also interesting to note that we have a finite growth rate at $k_r = 0$ at non-zero values of spanwise wave number. Now we will discuss the effect of spanwise wavenumber on the thermocapillary P mode instability. The spatial growth rates corresponding to P mode have been shown in (k_r, k_i) plane for various values of k_z when Re $= 10$, $M = 20$, and $B = 1$ in Fig. 6b. It can be noticed that the spatial growth rate increases significantly with the increment in spanwise wavenumber and hence it can be inferred that spanwise wavenumber has a destabilizing influence on the P mode instability. It is also interesting to note that the range of k_r within which the P mode instability occurs, shifts towards lower values of k_r significantly. It indicates that with the increment of spanwise wavenumber the P mode instability shifts towards long wave regime from short wave regime.

3.2 Inviscid Analysis

According to Squire's theorem, the two dimensional disturbances get unstable at lower values of Reynolds number compared to the three-dimensional ones [2]. Hence,
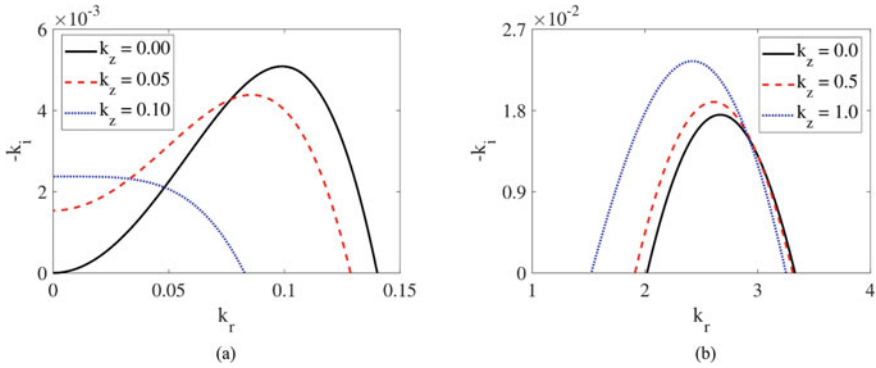
Fig. 6 **a** Evolution of spatial growth rate $-k_i$ for the S mode in (k_r, k_i) plane when Re $= 1$, and $M = 25$. **b** Evolution of spatial growth rate $-k_i$ for the P mode in (k_r, k_i) plane Re $= 10$ and $M = 20$. For both the plots $B = 1$

for performing inviscid stability analysis, we will consider two dimensional distur-bances only, that is, $k_z = 0$ and $k_x = k$. Now the perturbation velocity is converted to perturbation stream function ψ' as the flow is two-dimensional and it is considered to be in normal mode form

$$\psi' = \hat{v} \exp[ik(x - ct)]. \tag{9}$$

Now we will introduce two new parameters $W = $ We/Re and $m = $ Ma/Re which will be used equivalently for showing the effect of Weber number and Marangoni number. At inviscid limits, we will consider Reynolds number to be large (Re $\to \infty$) and inclination angle to be small ($\theta \to 0$). Therefore, in this limiting case, the OS-BVP (2)–(8) will take the following form

$$(\overline{U} - c)(D^2 - k^2)\hat{v} + \frac{2\hat{v}}{1 + 2\beta} = 0, \quad y \in [0, 1] \tag{10}$$

$$(\overline{U} - c)\hat{\tau} + \frac{\text{Bi}}{1 + \text{Bi}}\hat{v} = 0, \quad y \in [0, 1], \tag{11}$$

$$\hat{v} = 0, \quad \text{at } y = 0, \tag{12}$$

$$(c - \overline{U})^2 D\hat{v} - 2\left[k^2\left(W - \frac{m}{1 + \text{Bi}}\right) + \frac{2\cot\theta}{(1 + 2\beta)\text{Re}}\right]\hat{v} = 0, \quad \text{at } y = 0. \tag{13}$$

In Eq. (13) the term $2\cot\theta/\{(1 + 2\beta)\text{Re}\}$ is not neglected. This is due to the fact that although the value of 1/Re is small, the value of $\cot\theta$ will be large and hence the ratio $\cot\theta/\text{Re}$ will have a finite value. The complex wave speed is denoted by c $= c_r + ic_i$ in Eqs. (10)–(13) where c_r and c_i denotes the real and imaginary part of

c. Now to solve the second-order BVP (10)–(13), we will employ the transformation $\hat{v}(y) = (U - c)\Upsilon(y)$, which will lead to the following set of BVP

$$D\left[\left(\overline{U} - c\right)^2 D\Upsilon\right] - \left(\overline{U} - c\right)^2 k^2 \Upsilon = 0, \tag{14}$$

$$\left(\overline{U} - c\right)\left[\hat{\tau} + \frac{\text{Bi}}{1 + \text{Bi}}\Upsilon\right] = 0, \tag{15}$$

$$\Upsilon(0) = 0, \tag{16}$$

$$\left(\overline{U} - c\right)^2 D\Upsilon(1) = \left[\frac{2\cot\theta}{(1 + 2\beta)\text{Re}} + k^2\left(W - \frac{m}{1 + \text{Bi}}\right)\right]\Upsilon(1) \tag{17}$$

Note that here the Governing energy equation is not considered here as $\hat{\tau}$ can be directly predicted from Eq. (11). In order to solve the set of Eqs. (14)–(17), we will multiply it with Υ^*, the complex conjugate of Υ. After that Eq. (14) is integrated with respect to y when $y \in [0, 1]$ and the boundary conditions (16)–(17) are incorporated to get the following expression.

$$\int_0^1 \left(\overline{U} - c_r - ic_i\right)^2 P \, dy = \left[k^2\left(W - \frac{m}{1 + \text{Bi}}\right) + \frac{2\cot\theta}{\text{Re}(1 + 2\beta)}\right]|\Upsilon(1)|^2, \tag{18}$$

where $P = \left(k^2|\Upsilon(y)|^2 + |D\Upsilon(y)|^2\right) \geq 0$. Now, to compute the values of c_r and c_i, the real and imaginary parts of Eq. (18) are compared.

$$\int_0^1 \left[\left(\bar{U} - c_r\right)^2 - c_i^2\right] P \, dy = \left[k^2\left(W - \frac{m}{1 + \text{Bi}}\right) + \frac{2\cot\theta}{\text{Re}(1 + 2\beta)}\right]|\Upsilon(1)|^2, \tag{19}$$

$$c_i \int_0^1 \left(\overline{U} - c_r\right) P \, dy = 0. \tag{20}$$

Now for the shear mode to become unstable we should have $c_i > 0$. From Eq. (20), it can clearly be observed that for a non-trivial solution the unstable shear mode will not exist if $c_r > 1$. Therefore, for $c_r < 1$, we can have a solution for phase speed of unstable shear mode as

$$c_r = 1 - \left[1 - \frac{\int_0^1 (1 - y)^2 P \, dy}{(1 + 2\beta)\int_0^1 P \, dy}\right]. \tag{21}$$

Now from Eqs. (21) and (19) we get the expression for c_i as follows

$$c_i^2 = \frac{1}{(1+2\beta)^2}\left[\frac{\int_0^1 (1-y)^4 P\,\mathrm{d}y}{\int_0^1 P\,\mathrm{d}y} - \left(\frac{\int_0^1 (1-y)^2 P\,\mathrm{d}y}{\int_0^1 P\,\mathrm{d}y}\right)^2\right]$$
$$- \left[k^2\left(W - \frac{m}{1+\mathrm{Bi}}\right) + \frac{2\cot\theta}{\mathrm{Re}(1+2\beta)}\right]\frac{|\Upsilon(1)|^2}{\int_0^1 P\,\mathrm{d}y} \tag{22}$$

From the expression of c_i^2, we can clearly observe that with the increase in m the temporal growth rate related to shear mode increase. Therefore, we may conclude that Marangoni number has a destabilizing effect on the shear mode instability. This result is perfectly consistent with the results of Choudhury and Samanta [2].

4   Conclusion

Linear stability analysis of a liquid incompressible film flowing down an inclined plane has been performed. The inclined plane is considered to be uniformly heated and slippery. The liquid follows the Newton's law of viscosity. At the free surface or, the liquid–air interface the heat transfer is governed by the Newton's law of cooling. To carry out the spatial stability analysis, we have formulated a coupled set of OS-BVP type equations containing perturbation velocity and temperature. In order to estimate the spatial growth rate at arbitrary wave numbers, we have numerically solved the coupled set of equations employing Chebyshev collocation technique. Marangoni number is found to have a destabilizing influence on both the S and P modes. On the contrary, Biot number is found to have dual effect on S mode. At lower range ($B \leq 0.75$) although Biot number has a destabilizing effect on the S mode, at higher range ($B \geq 0.75$), it is found to have a stabilizing effect. Biot number exerts a stabilizing effect on thermocapillary P mode also. It has been observed that with the increase in spanwise wavenumber the spatial growth rate of S mode and P mode attenuates and intensifies respectively. We have also analytically solved the OS-BVP for the limiting case of inviscid flow where $\mathrm{Re} \to \infty$. In inviscid limit, the temporal growth rate for shear mode been evaluated which indicates a destabilizing effect of Marangoni number on the shear mode.

Nomenclature

Ma   Marangoni number [–]
Re   Reynolds number [–]
Bi   Biot number [–]
Pe   Peclet number [–]
We   Weber number [–]
Pr   Prandtl number [–]

k	Wavenumber [m^{-1}]
k_x	Streamwise wavenumber [m^{-1}]
k_z	Spanwise wavenumber [m^{-1}]
c	Wave speed [$m\,s^{-1}$]
ω	Angular sped [$rad\,s^{-1}$]
θ	Inclination angel [rad]
σ	Surface tension coefficient [$N\,m^{-1}$]
φ	Perturbation velocity amplitude [$m\,s^{-1}$]
τ	Perturbation temperature amplitude [K]
η	Perturbation film thickness [m]
Ψ'	Perturbation streamfunction [$m^2\,s^{-1}$]
β	Dimensionless slip length [–]
T_a	Ambient temperature [K]
T_w	Wall temperature [K]

References

1. Bhat FA, Samanta A (2018) Linear stability of a contaminated fluid flow down a slippery inclined plane. Phys Rev E 98(3):033108
2. Choudhury A, Samanta A (2022) Linear stability of a falling film over a heated slippery plane. Phys Rev E 105(6):065112
3. Goussis DA, Kelly RE (1990) On the thermocapillary instabilities in a liquid layer heated from below. Int J Heat Mass Transfer 33:2237–2245
4. Hu J, Hadid HB, Henry D, Mojtabi A (2008) Linear temporal and spatio-temporal stability analysis of a binary liquid film flowing down an inclined uniformly heated plate. J Fluid Mech 599:269–298
5. Kalliadasis S, Ruyer-Quil C, Scheid B, Velarde MG (2012) Falling liquid films. Springer
6. Lin SP (1967) Instability of a liquid film flowing down an inclined plane. Phys Fluids 10:308–313
7. Lin SP (1975) Stability of liquid flow down a heated inclined plane. Lett Heat Mass Transfer 2:361–369
8. Pascal JP, D'Alessio SJD (2016) Thermosolutal Marangoni effects on the inclined flow of a binary liquid with variable density. I. Linear stability analysis. Phys Rev Fluids 1(8):083603
9. Samanta A (2013) Shear wave instability for electrified falling films. Phys Rev E 88(5):053002